

Is the $X(3872)$ a bound state ?

Pablo G. Ortega¹⁾ Enrique Ruiz Arriola²⁾

¹ Grupo de Física Nuclear and Instituto Universitario de Física Fundamental y Matemáticas (IUFFyM), Universidad de Salamanca, E-37008 Salamanca, Spain

² Departamento de Física Atómica, Molecular y Nuclear

and Instituto Carlos I de Física Teórica y Computacional, Universidad de Granada, E-18071 Granada, Spain.

Abstract: All existing experimental evidence of the bound state nature of the $X(3872)$ relies on considering its decay products with a finite experimental spectral mass resolution which is typically $\Delta m \geq 2\text{MeV}$ and much larger than its alleged binding energy, $B_X = 0.00(18)\text{MeV}$. On the other hand, we have found recently that there is a neat cancellation in the 1^{++} channel for the invariant $D\bar{D}^*$ mass around the threshold between the continuum and bound state contribution. This is very much alike a similar cancellation in the proton-neutron continuum with the deuteron in the 1^{++} channel. Based on comparative fits of experimental cross section deuteron and $X(3872)$ prompt production in pp collisions data with a finite p_T to a common Tsallis distribution we find a strong argument questioning the bound state nature of the state but also explaining the large observed production rate likely consistent with a half-bound state.

Key words: Charmonium molecular states, Particle Production, Tsallis distribution

PACS: 12.39.Pn, 14.40.Lb, 14.40.Rt

1 Introduction

The early possibility of loosely bound states near the charm threshold first envisaged in Ref. [1] seems to be confirmed now by the wealth of evidence on the existence of the $X(3872)$ state with binding energy $B_X = M_D + M_{\bar{D}^*} - M_X = 0.00(18)\text{MeV}$ [2] and which has triggered a revolution by the proliferation of the so-called X,Y,Z states (for reviews see e.g. [3, 4]). In the absence of electroweak interactions this state has the smallest known hadronic binding energy. However, since this state is unstable, all the detection methods of the $X(3872)$ are based on looking for its decay channels spectra such as $X \rightarrow J/\psi\pi^+\pi^-$ where the mass resolution never exceeds $\Delta m \sim 1 - 2\text{MeV}$ [5–8] (see e.g. [9] for a pictorial display on spectral experimental resolution). Therefore it is in principle unclear if one can determine the mass of the $X(3872)$ or equivalently its binding energy $\Delta B_X \ll \Delta m$ with such a precision, since we cannot distinguish sharply the initial state.

In most analyses up to now (see however [10]) the bound state nature is assumed rather than deduced. In fact, the molecular interpretation has attracted considerable attention, since for a loosely bound state many properties are mainly determined by its binding energy [4] and characterized by a line shape in production processes [11]. However, we have noticed recently a neat and accurate cancellation between the would-be $X(3872)$ bound state and the $D\bar{D}^*$ continuum which has a sizable impact on the occupation number at finite temperature [12, 13]. This reduction stems from a cancellation in the density of states in the 1^{++} channel and potentially blurs any detected signal where a superposition of 1^{++} states

is at work. Such a circumstance makes us questioning in the present letter the actual character of the state. We will do so by analyzing the p_T distribution of the $X(3872)$ in high energy production experiments and folding the expected distribution with the actual mass distribution corresponding to the 1^{++} spectrum via the level density within the accessible experimental resolution. For our argument a qualitative and quantitative comparison with a truly weakly bound state such as the deuteron, d , will be most enlightening. As a matter of fact, the similarities between d and $X(3872)$ have been inspiring [14–16]. Compared to the $X(3872)$ the main difference is that the deuteron is detected *directly* by analyzing its well defined track and/or stopping power. Actually, the production of loosely bound nuclei and anti-nuclei, including $d, \bar{d}, {}^3\text{He}_\Lambda$, etc. in ultra-high pp collisions is a remarkable and surprising experimental observation in recent years [17] and so far poorly understood [18].

The cancellation echoes a similar effect on the deuteron pointed out by Dashen and Kane in their discussion on the counting of states in the hadron spectrum in a coarse grained sense [19] which we review in some detail in the next section. In section 3 we analyze the consequences in a production process. Finally, in section 4 we draw our the conclusions and provide an outlook for future work.

2 Dashen and Kane cancellation mechanism

In order to illustrate the Dashen-Kane mechanism [19] we introduce the cumulative number of states with invariant CM mass \sqrt{s} below M in a given channel with fixed J^{PC} quantum numbers. This involves the J^{PC} spectrum which contains

1) E-mail: pgortega@usal.es

2) E-mail: earriola@ugr.es

bound states and continuum states with threshold M_{th} and is given as

$$N(M) = \sum_i \theta(M - M_i^B) + \frac{1}{\pi} \sum_{\alpha=1}^n [\delta_{\alpha}(M) - \delta_{\alpha}(M_{\text{th}})]. \quad (1)$$

where the index i runs over the M_i^B bound states and α over the n coupled channels. Here we have separated bound states M_i^B explicitly from scattering states written in terms of the eigenvalues of the S-matrix, i.e. $S = U \text{Diag}(e^{2i\delta_1}, \dots, e^{2i\delta_n}) U^\dagger$, with U a unitary transformation for n -coupled channels and $\delta_i(M)$ the eigenphaseshifts for the channel i at CM invariant mass $\sqrt{s} = M$. This definition fulfills $N(0) = 0$. In the single channel case, and in the limit of high masses $M \rightarrow \infty$ one gets $N(\infty) = n_B + \frac{1}{\pi} [\delta(\infty) - \delta(M_{\text{th}})] = 0$ due to Levinson's theorem. While the origin of the bound state term is quite obvious, the derivation of the continuum term is a bit subtle but standard and can be found in many textbooks on statistical mechanics dealing with the quantum virial expansion (see e.g. [20, 21]). In potential scattering it can be best deduced by confining the system in a large spherical box which quantizes the energy and relates the energy shift due to the interaction to the phase-shift and then letting the volume of the system go to infinity [19].

In the particular case of the deuteron, which is a neutron-proton 1^{++} state bound by $B_d = 2.2 \text{ MeV}$, the cancellation between the continuum and discrete parts of the spectrum was pointed out by Dashen and Kane long ago [19]. (see also [22, 23] for an explicit picture and further discussion within the resonance gas model framework). The opening of new channels and the impact of confining interactions was discussed in Ref. [24]. In the 1^{++} channel, the presence of tensor force implies a coupling between the 3S_1 and 3D_1 channels. While the partial wave analysis of NN scattering data and the determination of the corresponding phase-shifts is a well known subject [25], we note that a similar analysis in the $D\bar{D}^*$ case is at present in its infancy. In our first model determination in Ref. [12, 13] the mixing has an influence for larger energies than those considered here. Therefore, in order to illustrate how the cancellation comes about, we consider a simple model which works sufficiently accurately for *both* the deuteron and the $X(3872)$ by just considering a contact (gaussian) interaction [26] in the 3S_1 -channel and using effective range parameters to determine the corresponding phase-shift in the d and $X(3872)$ channels [12, 27] respectively.

The result for $N(M)$ in both d or X cases depicted in Fig. 1 display a similar pattern for the np or $D\bar{D}^*$ invariant masses respectively. The sharp rise of the cumulative number is followed by a strong decrease generated by the phase-shift. For larger invariant masses M several effects appear, and in particular the nuclear core (see e.g. [23]) or composite nature of the $X(3872)$ and its $c\bar{c}$ content becomes manifest (see e.g. [28]).

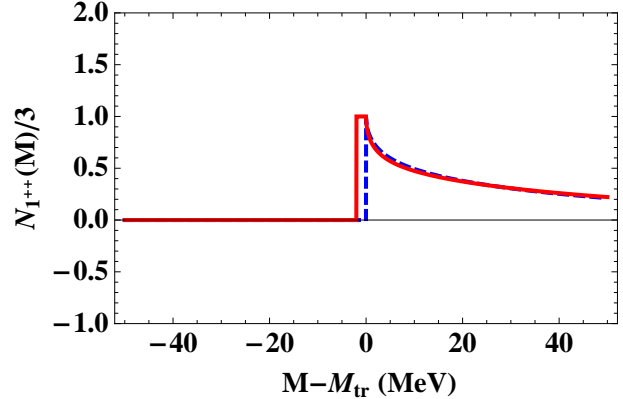


Figure 1. Cumulative number in the 1^{++} channel for the deuteron (solid) and $X(3872)$ (dashed) as a function of the invariant mass M respect to np and $D\bar{D}^*$ values respectively. We divide by spin degeneracy.

An immediate consequence of this effect trivially follows from Eq. (1) for an observable depending on the invariant mass function $O(M)$. The corresponding measured quantity for a bin in the range $(m - \Delta m/2, m + \Delta m/2)$ becomes

$$O_{\Delta m} \equiv \int_{m - \Delta m/2}^{m + \Delta m/2} dM \rho(M) O(M). \quad (2)$$

where $\rho(M)$ is the density of states, defined as

$$\rho(M) = \frac{dN(M)}{dM} = \sum_i \delta(M - M_i^B) + \frac{1}{\pi} \sum_{\alpha=1}^n \delta'_{\alpha}(M), \quad (3)$$

where $\delta'_{\alpha}(M)$ denotes the derivative of the phase shift with respect to the mass.

In the single channel case, with phase shift $\delta_{\alpha}(M)$, and if the resolution is much larger than the binding energy $\Delta m \gg |B| \equiv |M_B - M_{\text{tr}}|$ one has

$$O|_{M^B \pm \Delta m} = O(M^B) + \frac{1}{\pi} \int_{M_{\text{tr}}}^{M_{\text{tr}} + \Delta m/2} dM \delta'_{\alpha}(M) O(M). \quad (4)$$

which, on view of Fig. 1 and for a smooth observable $O(M)$, points to the cancellation, anticipated by Dashen and Kane [24]. The effect was explicitly seen in the np virial coefficient at astrophysical temperatures, $T \sim 1 - 10 \text{ MeV}$ [29]. We have recently shown [12] how this cancellation can likewise be triggered for the $X(3872)$ occupation number at quark-gluon crossover temperatures $T \sim 100 - 200 \text{ MeV}$. This will be relevant in relativistic heavy ion collisions when X -production yields are measured, because the partition function involves a Boltzmann factor, $\sim e^{-\sqrt{p^2 + m^2}/T}$ with the density of states, Eq. (3) and the measured yields reproduce remarkably the predictions occupation numbers in the hadron resonance gas model [30].

Therefore, given these tantalizing similarities a comparative study of the deuteron and $X(3872)$ production rates to ultra-high energies in colliders provides a suitable calibration

tool in order to see the effects of the Dashen-Kane cancellation due to the finite resolution Δm of the detectors signaling the $X(3872)$ state via its decay products and decide on its bound state character. Here we propose to study the effect in the observed transverse momentum (p_T) distributions.

3 $X(3872)$ production abundance

While the theory regarding the shape of transverse momentum distribution is not fully developed (see e.g. Ref. [31] for an early review, Ref. [32] for a historical presentation), we will rest on phenomenological ansatze which describe the data. On the one hand, the asymptotic p_T -spectrum [33] provides a production rate $1/p_T^8$ based on quark-quark scattering. Hagedorn realized that an interpolation between the power correction and a thermal Boltzmann p_T -distribution would work [34]. A thermodynamic interpretation for non-extensive systems [35] of the rapidity distribution was proposed by Tsallis [36] and first applied to high energy phenomena in Refs. [37, 38], namely the differential occupation number is given by

$$\frac{d^3N}{d^3p} = \frac{gV}{(2\pi)^3} \left(1 + (q-1)\frac{E(p)}{T}\right)^{-\frac{q}{q-1}} \xrightarrow{q \rightarrow 1} \frac{gV}{(2\pi)^3} e^{-\frac{E(p)}{T}} \quad (5)$$

where $E(p) = \sqrt{p^2 + m^2}$, V is volume of the system, T the temperature and g the degrees of freedom and, as indicated, the limit $q \rightarrow 1$ produces the Boltzmann distribution. We use here the form obtained by the maximum Tsallis entropy principle [39].

The invariant differential production rate, $d^3N/(d^2p_T dy) \equiv E_p d^3N/d^3p$ with $y = \tanh^{-1}(E_p/p_z)$ the rapidity, has the asymptotic matching corresponds to $q = 1.25$ [40]. While the thermodynamic interpretation is essential to link the degrees of freedom g with the production rate [41], we note that we have checked [42] that a Tsallis distribution describes accurately the results from particle Monte Carlo generators such as PYTHIA [43, 44]. This distribution has also been applied recently by the ALICE collaboration to d -production [45] in pp collisions.

We show next that the $X(3872)$, $\Psi(2S)$ and deuteron prompt production cross sections can be described with the same Tsallis distribution:

$$\frac{1}{2\pi p_T} \frac{d\sigma(m)}{dp_T} = \mathcal{N} \int dy E(p_T, y) \left[1 + \frac{q-1}{T} E(p_T, y)\right]^{\frac{q}{1-q}} \quad (6)$$

with $E(p_T, y) = \sqrt{p_T^2 + m^2} \cosh y$ and \mathcal{N} a normalization factor. Obviously, a direct comparison requires similar p_T values as possible for both d , $\Psi(2S)$ and $X(3872)$; the closest ones come from ALICE [45] and CMS [46, 47] respectively. The ATLAS data for $X(3872)$ [48] confirm a power law behaviour in p_T but extend over a much larger range than the available d and hence are not used in this study. The deuteron data is given in invariant differential

yields $d^2N/(2\pi p_T dp_T dy)$, hence the inelastic pp cross section at $\sqrt{s} = 7$ TeV, $\sigma_{\text{inel}}^{pp} = 73.2 \pm 1.3$ mb, as measured by TOTEM [49] has been used to transform it into differential cross section.

Table 1. Best fit of parameters for Tsallis distribution. The X data used from CMS [47] is multiplied by the branching fraction $\mathcal{B}_X \equiv \mathcal{B}(X \rightarrow J/\psi \pi^+ \pi^-)$. Correlation between q and T parameters is practically -1 ($r = -0.9992$).

	$X(3872) + d$	$X(3872) + \Psi(2S) + d$
$\ln(\mathcal{N}_X \mathcal{B}_X)$	41.4 ± 0.4	41.4 ± 0.4
$\ln(\mathcal{N}_d)$	40.35 ± 0.09	40.35 ± 0.09
$\ln(\mathcal{N}_\Psi)$	-	44.3 ± 0.2
q	1.122 ± 0.001	1.122 ± 0.001
T [MeV]	7.017 ± 0.07	7.018 ± 0.07
N_d	$(2.02 \pm 0.02) \cdot 10^{-4}$	$(2.01 \pm 0.02) \cdot 10^{-4}$
$N_X \mathcal{B}_X$	$(9 \pm 3) \cdot 10^{-6}$	$(9 \pm 3) \cdot 10^{-6}$
N_Ψ	-	$(2.2 \pm 0.3) \cdot 10^{-4}$
$\langle p_T \rangle_d$	1.102 ± 0.007	1.102 ± 0.007
$\langle p_T \rangle_X$	2.249 ± 0.015	2.249 ± 0.015
$\langle p_T \rangle_\Psi$	2.142 ± 0.014	2.142 ± 0.014
$N_X \mathcal{B}_X / N_d$	$0.046_{-0.013}^{+0.016}$	$0.046_{-0.013}^{+0.015}$
N_Ψ / N_d	-	$1.09_{-0.17}^{+0.16}$

On a phenomenological level we perform two fits: One including d and $X(3872)$ data and another one adding the $\Psi(2S)$ data. In both cases the $\mathcal{N}_{d,X,[\Psi]}$, q and T are fitted by minimizing the corresponding χ^2 function with Minuit [50]. The experimental error in the x -axis has been incorporated in the χ^2 via a MonteCarlo procedure with 5000 runs, where the p_T value of each experimental data has been randomly shifted within the experimental range with an uniform distribution. Due to the scarcity of X data, we assume the production rate is mainly driven by the deuteron. That way, an initial minimization of the q , T and \mathcal{N}_d is done, and the resulting best-fit values of q and T are employed to fix \mathcal{N}_X and \mathcal{N}_Ψ .

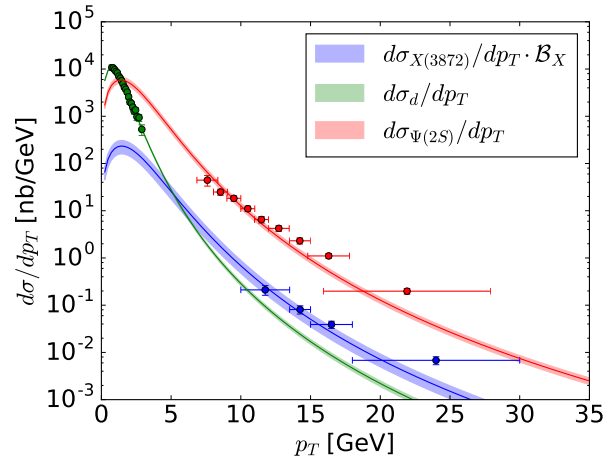


Figure 2. Comparison between the prompt production cross section in pp collisions of $X(3872)$ (blue), the deuteron (green) and the $\Psi(2S)$ (red). $\Psi(2S)$ data from CMS [46]. The $X(3872)$ data from CMS [47] is

multiplied by the branching fraction $\mathcal{B}(X \rightarrow J/\psi\pi\pi)$. Deuteron data in pp collisions are taken from ALICE [45]. The lines are Tsallis distributions fitted to each data set, with the same q and T parameters. We fit both $X(3872)$, $\Psi(2S)$ and deuteron data. The shadowed bands represent the statistical 68% confidence level (CL) obtained from the fit.

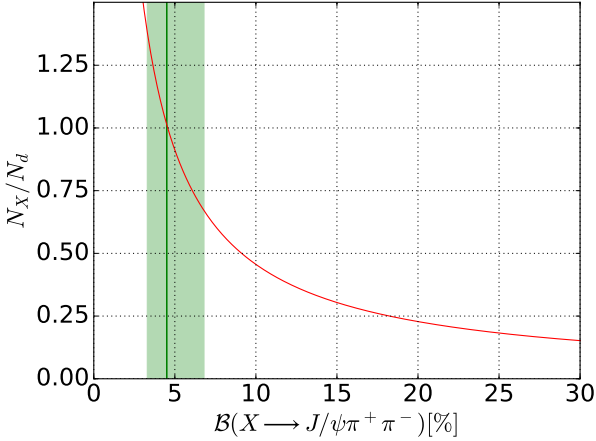


Figure 3. In red, the $X(3872)$ vs deuteron prompt production ratio as a function of the branching fraction $\mathcal{B}(X \rightarrow J/\psi\pi^+\pi^-)$ when fitting to $X(3872)$, $\Psi(2S)$ and deuteron data. The shadowed band represent the statistical 68% confidence level (CL) obtained from the fit. The green band shows the constrains of the recent analysis of C. Li *et al* from BESIII data [51] $\mathcal{B}_X \equiv \mathcal{B}(X \rightarrow J/\psi\pi^+\pi^-) = 4.5^{+2.3}_{-1.2}$.

The results can be found in Tab. 1, and the final production fit at Fig. 2 for the two considered calculations, one with the $X(3872)$ and the deuteron, and another for the $X(3872)$, the $\Psi(2S)$ and the deuteron. They are both compatible, as expected, as the X to $\Psi(2S)$ production ratio, measured at CMS, is almost constant [47]. The X/d production ratio is $0.046^{+0.016}_{-0.013}$ for $X + d$ fit (and practically the same value for $X + \Psi + d$ fit), dependent on the value of the branching fraction. Note that we do not have the pure cross section for the X , as it is multiplied by the unmeasured branching fraction which has been recently constrained in an analysis of BESIII data by C. Li *et al* [51] to be $\mathcal{B}_X \equiv \mathcal{B}(X \rightarrow J/\psi\pi^+\pi^-) = 4.5^{+2.3}_{-1.2}\%$. This value is consistent with the PDG lower- $\mathcal{B}_X > 3.2\%$ [52], and upper bound $\mathcal{B}_X < 6.6\%$ at 90% C.L. [53]. The uncertainty comes from the most recent value of $\mathcal{B}_X \cdot (B^- \rightarrow K^- X(3872)) < 2.6 \times 10^{-4}$ at 90% C.L. [54]. We note that in a recent paper, Esposito *et al.* [55] consider the wider range $8.1^{+1.9}_{-3.1}\%$.

Consequently, we can study the ratio of the X/d occupation numbers as a function of the \mathcal{B}_X branching fraction. In Fig. 3 we see the results. Considering the error bars, the experimental constrains give ratios between 0.3 and 1.9 for N_X/N_d .

In our previous fits above we have neglected the role played by the finite resolution of the detectors, Δm , which we discuss next. Ref. [47] uses a $\pm 2\sigma$ window around the $X(3872)$ mass, with $\sigma = 5 - 6$ MeV, to select the $X(3872)$ events in the $J/\psi\pi\pi$ invariant mass spectrum. That means that the branching fraction $\mathcal{B}(X \rightarrow J/\psi\pi^+\pi^-)$, as measured by CMS is averaged in the $[M_X - 2\sigma, M_X + 2\sigma]$ energy window, which includes the continuum. As a consequence of the energy window, there are many decays that can be affected, those involving the $\bar{D}^0 D^{0*}$ channel.

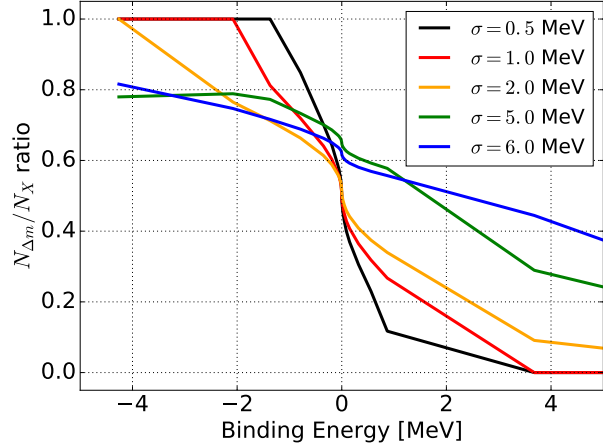


Figure 4. The relative occupation number *with* and *without* finite resolution $\Delta m = 2\sigma$ as a function of the $X(3872)$ binding energy. Using $M_X = M_D + M_{\bar{D}^*} - \gamma_X^2/(2\mu_{D,\bar{D}^*})$ we take the positive branch for the virtual state ($\gamma_X > 0$) and the negative branch for the bound state ($\gamma_X < 0$) for different σ values.

In fact, the distribution obtained from Eq. 5 depends on the mass, and hence its observed value undergoes formula 4, reflecting the finite resolution. Similar to the finite temperature case [12] we have checked that the Tsallis p_T -shape is basically preserved for $p_T \gg \Delta m$, but the occupation number is modified for $\Delta m \gg B$.

For definiteness we use $\Delta m = 2\sigma$, as CMS measures the $X(3872)$ in a $\pm 2\sigma$ region around the central value of the X mass. The net effect is summarized in a ratio, which we find to be practically independent of the transverse momentum p_T for the Tsallis distribution shape,

$$\frac{\sigma_{m=M_X \pm \Delta m}}{\sigma_{M_X}} \sim \frac{\mathcal{N}_{\Delta m}}{\mathcal{N}_X}. \quad (7)$$

This formula will allow us to set values for the relative occupation numbers due to the finite resolution. We take $M_X = M_D + M_{\bar{D}^*} - \gamma_X^2/(2\mu_{D,\bar{D}^*})$ as a parameter by looking at the poles of the $D\bar{D}^*$ S-matrix in the ${}^3S_1 - {}^3D_1$ channel [12]. Therefore, while in the limit of $\Delta m \rightarrow 0$ we should expect the ratio $N_X/N_d \rightarrow 1, 1/2$ or 0 for a bound ($\gamma_X > 0$), half-bound ($\gamma_X = 0$) or unbound (actually virtual, ($\gamma_X < 0$)) state, for increasing and finite Δm the value lies somewhat in between and

the different situations can be hardly distinguished. However, as seen in Fig. 4 the numerical value $N_{\Delta m}/N_X \sim 0.5 - 0.6$ is rather stable for a reasonable range of B_X and σ values. If we re-interpret N_X as $N_{X,\Delta m}$ this falls remarkably in the bulk of Fig. 3 where $N_{X,\Delta m}/N_d \sim 0.5$ implies $N_X/N_d \sim 1$. Thus, unlike expectations, we *do not* find the production rate to change dramatically due to binding energy effects due to Δm ; the p_T shape will likewise not depend on this (unlike expectations [55]). In a recent and insightful paper Kang and Oller have analyzed the character of the $X(3872)$ in terms of bound and virtual states within simple analytical parameterizations [10]. While the Dashen-Kane cancellation has not been explicitly identified, it would be interesting to see if their trends can be reproduced by more microscopic approaches.

4 Conclusions

Theoretically, it is appealing an scenario where the $X(3872)$ is a half-bound state (zero binding energy) corre-

One of us (E.R.A.) thanks Airton Deppman for discussions on Tsallis distributions. This work is partly supported by the Spanish Ministerio de Economía y Competitividad

sponding to the so-called unitarity limit, characterized by scale invariance [56]. In this case, the phase-shift becomes $\delta = \pi/2$ around threshold, and the occupation number becomes a half of that of the bound state. Our analysis shows that the large production rate of the $X(3872)$ at finite p_T does not depend strongly on the details of the binding since the experimental bin size is much larger than the binding energy. We also find striking and universal shape similarities with the $\psi(2S)$ and deuteron production data via a common Tsallis distribution. A more direct check of our predicted mild suppression might be undertaken if all production data would be within the same p_T values. Finally, we note that in order to envisage a clear fingerprint of the $X(3872)$ binding character a substantial improvement on the current experimental resolution of its decay products would be required.

References

- 1 S. Nussinov and D.P. Sidhu, Nuovo Cim. A44 (1978) 230.
- 2 Particle Data Group, M. Tanabashi et al., Phys. Rev. D98 (2018) 030001.
- 3 A. Esposito, A. Pilloni and A.D. Polosa, Phys. Rept. 668 (2016) 1, 1611.07920.
- 4 F.K. Guo et al., Rev. Mod. Phys. 90 (2018) 015004, 1705.00141.
- 5 Belle, S.K. Choi et al., Phys. Rev. Lett. 91 (2003) 262001, hep-ex/0309032.
- 6 BaBar, B. Aubert et al., Phys. Rev. D71 (2005) 031501, hep-ex/0412051.
- 7 S.K. Choi et al., Phys. Rev. D84 (2011) 052004, 1107.0163.
- 8 LHCb, R. Aaij et al., Phys. Rev. Lett. 110 (2013) 222001, 1302.6269.
- 9 M. Karliner, J.L. Rosner and T. Skwarnicki, (2017), 1711.10626.
- 10 X.W. Kang and J.A. Oller, Eur. Phys. J. C77 (2017) 399, 1612.08420.
- 11 F.K. Guo, Phys. Rev. Lett. 122 (2019) 202002, 1902.11221.
- 12 P.G. Ortega, D. R. Entem, F. Fernández, E. Ruiz Arriola, Phys. Lett. B781 (2018) 678, 1707.01915.
- 13 P.G. Ortega and E. Ruiz Arriola, PoS Hadron2017 (2018) 236, 1711.10193.
- 14 N.A. Tornqvist, Z. Phys. C61 (1994) 525, hep-ph/9310247.
- 15 F.E. Close and P.R. Page, Phys. Lett. B578 (2004) 119, hep-ph/0309253.
- 16 E. Braaten and M. Kusunoki, Phys. Rev. D69 (2004) 074005, hep-ph/0311147.
- 17 P. Braun-Munzinger and B. Dönigus, Nucl. Phys. A987 (2019) 144, 1809.04681.
- 18 Y. Cai et al., (2019), 1905.02753.
- 19 R.F. Dashen and G.L. Kane, Phys. Rev. D11 (1975) 136.
- 20 G. Parisi, ‘Statistical Field Theory,’ REDWOOD CITY, USA: ADDISON-WESLEY (1988) 352 P. (FRONTIERS IN PHYSICS, 66)
- 21 K. Huang, Introduction to statistical physics, Chapman and Hall/CRC (2009)
- 22 E. Ruiz Arriola, L.L. Salcedo and E. Megias, Acta Phys. Polon. Supp. 8 (2015) 439, hep-ph/1505.02922.
- 23 E. Ruiz Arriola, L.L. Salcedo and E. Megias, Acta Phys. Polon. B45 (2014) 2407, hep-ph/1410.3869.
- 24 R.F. Dashen, J.B. Healy and I.J. Muzinich, Phys. Rev. D14 (1976) 2773.
- 25 R. Navarro Prez, J.E. Amaro and E. Ruiz Arriola, Phys. Rev. C88 (2013) 064002, 1310.2536, [Erratum: Phys. Rev.C91,no.2,029901(2015)].
- 26 D. Gamermann, J. Nieves, E. Ruiz Arriola and E. Oset Phys. Rev. D81 (2010) 014029, hep-ph/0911.4407.
- 27 E. Ruiz Arriola, S. Szpigel and V.S. Timoteo, Phys. Lett. B728 (2014) 596, nucl-th/1307.1231.
- 28 P.G. Ortega et al., Phys. Rev. D81 (2010) 054023, hep-ph/0907.3997.
- 29 C.J. Horowitz and A. Schwenk, Nucl. Phys. A776 (2006) 55, nucl-th/0507033.
- 30 A. Andronic et al., Nature 561 (2018) 321, 1710.09425.
- 31 D.W. Sivers, S.J. Brodsky and R. Blankenbecler, Phys. Rept. 23 (1976) 1.
- 32 J. Rak and M.J. TannenbaumHigh p_T physics in the heavy ion era Vol. 34 (Cambridge University Press, 2013).
- 33 R.P. Feynman, R.D. Field and G.C. Fox, Phys. Rev. D18 (1978) 3320, [,739(1978)].
- 34 R. Hagedorn, Riv. Nuovo Cim. 6N10 (1983) 1.
- 35 H. Feshbach, Physics Today 40 (1987) 9.
- 36 C. Tsallis, Possible Generalization of Boltzmann-Gibbs Statistics, 1988.
- 37 I. Bediaga, E.M.F. Curado and J.M. de Miranda, Physica A286 (2000) 156, hep-ph/9905255.
- 38 W.M. Alberico, A. Lavagno and P. Quarati, Eur. Phys. J. C12 (2000) 499, nucl-th/9902070.
- 39 E. Megias, D.P. Menezes and A. Deppman, Physica A421 (2015) 15.
- 40 T. Bhattacharyya et al., Eur. Phys. J. A54 (2018) 222, 1712.08334.
- 41 J. Cleymans and D. Worku, Eur. Phys. J. A48 (2012) 160, 1203.4343.
- 42 P. G. Ortega and E. Ruiz Arriola, Work in preparation .
- 43 T. Sjostrand, S. Mrenna and P.Z. Skands, Comput. Phys. Commun. 178 (2008) 852, 0710.3820.

- 44 T. Sjostrand, S. Mrenna and P.Z. Skands, JHEP 05 (2006) 026, hep-ph/0603175.
- 45 ALICE, S. Acharya et al., Phys. Rev. C97 (2018) 024615, 1709.08522.
- 46 CMS, S. Chatrchyan et al., JHEP 02 (2012) 011, 1111.1557.
- 47 CMS, S. Chatrchyan et al., JHEP 04 (2013) 154, 1302.3968.
- 48 ATLAS, M. Aaboud et al., JHEP 01 (2017) 117, 1610.09303.
- 49 TOTEM, G. Antchev et al., EPL 101 (2013) 21004.
- 50 F. James and M. Roos, Comput. Phys. Commun. 10 (1975) 343.
- 51 C. Li and C. Z. Yuan, arXiv:1907.09149 [hep-ex].
- 52 Particle Data Group, C. Patrignani et al., Chin. Phys. C40 (2016) 100001.
- 53 Belle, C.Z. Yuan, 29th International Conference on Physics in Collision (PIC 2009) Kobe, Japan, August 30-September 2, 2009, 2009, 0910.3138.
- 54 Belle, Y. Kato et al., Phys. Rev. D97 (2018) 012005, 1709.06108.
- 55 A. Esposito et al., Phys. Rev. D92 (2015) 034028, 1508.00295.
- 56 G.A. Baker, Phys. Rev. C60 (1999) 054311.